# LABORATORY INFRARED SPECTRA OF POLYCYCLIC AROMATIC NITROGEN HETEROCYCLES: QUINOLINE AND PHENANTHRIDINE IN SOLID ARGON AND $H_2O$

M. P. Bernstein,[1] A. L. Mattioda,[1,2] S. A. Sandford,[1] and D. M. Hudgins[1]

## ABSTRACT

Polycyclic aromatic hydrocarbons (PAHs) are common throughout the universe. Their detection and identification are based on the comparison of IR observations with laboratory spectra. Polycyclic aromatic nitrogen heterocycles (PANHs) are heterocyclic aromatics, i.e., PAHs with carbon atoms replaced by a nitrogen atom. These molecules should be present in the interstellar medium, but have received relatively little attention. We present mid-IR spectra of two PANHs, quinoline ($C_9H_7N$) and phenanthridine ($C_{13}H_9N$), isolated in solid argon and frozen in solid $H_2O$ at 15 K, conditions yielding data directly comparable to astronomical observations. Quinoline and phenanthridine have been detected in meteorite extracts, and in general these nitrogen heterocycles are of astrobiological interest, since this class of molecules includes nucleobases, basic components of our nucleic acids. In contrast to simple PAHs, which do not interact strongly with solid $H_2O$, the nitrogen atoms in PANHs are potentially capable of hydrogen bonding with $H_2O$. Whereas the IR spectrum of phenanthridine in $H_2O$ is similar to that of the same compound isolated in an argon matrix, quinoline absorptions shift up to 16 cm$^{-1}$ (0.072 $\mu$m) between argon and $H_2O$. Thus, astronomers will not always be able to rely on IR band positions of matrix-isolated PANHs to correctly interpret the absorptions of PANHs frozen in $H_2O$ ice grains. Furthermore, our data suggest that relative band areas also vary, so determining column densities to better than a factor of 3 will require knowledge of the matrix in which the PANH is embedded and laboratory studies of relevant samples.

*Subject headings:* infrared: ISM — ISM: clouds — ISM: lines and bands — ISM: molecules — line: formation — molecular data

## 1. INTRODUCTION

Based on infrared (IR) astronomy, aromatic molecules are thought to be ubiquitous in the interstellar medium (ISM) and, as a class, the most common organic compounds in the universe (Snow & Witt 1995; Cox & Kessler 1999). IR spectra of polycyclic aromatic hydrocarbons (PAHs) and their cations, isolated in inert gas matrices, have been employed to fit astronomical observations of IR *emission* from gas-phase PAHs (Allamandola et al. 1999; Peeters et al. 2002) and exploit them as probes of interstellar emission zones. IR *absorptions* of aromatic molecules along lines of sight that include cold dust and ice (Smith et al. 1989; Sellgren et al. 1995; Brooke et al. 1999; Chiar et al. 2000; Bregman et al. 2000; Bregman & Temi 2001) suggest that aromatics might be intimately mixed with solid $H_2O$.

In a previous paper, we measured IR spectra of the smallest PAH, naphthalene ($C_{10}H_8$), in solid $H_2O$ at various temperatures and concentrations (Sandford et al. 2004). Compared to the spectra of naphthalene in argon matrices, we saw only modest changes in the IR spectra of naphthalene in $H_2O$: modest band shifts (typically less than 5 cm$^{-1}$), increased bandwidths (factors of 1.5–3), and changes in relative band strengths (typically less than a factor of 2–3). In a second paper (Bernstein et al. 2005), we demonstrate that a wide variety of other PAHs show the same spectral behaviors.

In this paper, we extend our laboratory spectroscopy of species under astrophysically relevant conditions to include polycyclic aromatic nitrogen heterocycles (PANHs)—PAHs bearing a nitrogen in the ring structure in place of a carbon atom. These compounds are present in meteorites (Stoks & Schwartz 1982;

Basile et al. 1984; Pizzarello 2001; Sephton 2002), are predicted to be a component of Titan's haze (Ricca et al. 2001), and, as a class, should be present in the ISM (Mattioda et al. 2003; Hudgins & Allamandola 2004), albeit at a lower abundance than their normal PAH counterparts (Kuan et al. 2003). Moreover, this type of compound is of astrobiological interest because it includes prebiotically significant species such as nucleobases (Peeters et al. 2003).

Quinoline ($C_9H_7N$) is a two-ring aromatic compound structurally analogous to naphthalene, but having a nitrogen atom in place of a carbon atom adjacent to the ring fusion (see structure in Fig. 1). Phenanthridine ($C_{13}H_9N$) is a three-ring aromatic compound structurally analogous to phenanthrene, but having a nitrogen atom in the outside edge of the central ring (see structure in Fig. 7). Both of these compounds have been detected in meteorite extracts. In contrast to simple carbon- and hydrogen-containing PAHs that do not interact strongly with $H_2O$ (Sandford et al. 2004; Bernstein et al. 2005), the nitrogen atom(s) in PANHs are potentially capable of hydrogen bonding with $H_2O$ or $CH_3OH$. This could lead to more interesting and complicated spectra for these molecules when they are present in astrophysical ices, particularly $H_2O$. A full theoretical treatment of the inter- and intramolecular interactions giving rise to the differences between the spectra of PANHs in an argon matrix and $H_2O$ will be presented elsewhere (D. E. Woon et al. 2005, in preparation). In this paper we focus on the aspects of the laboratory spectroscopy of PANHs of relevance to the astronomical community.

Although IR astronomy has been used to identify specific gas-phase molecules and simple molecules in the solid state, it cannot identify a specific complex organic molecule in the solid phase. On the other hand, it is the only way to probe the grains, where we expect these molecules to be; just as there can be a

---

[1] NASA-Ames Research Center, MS 245-6, Moffett Field, CA 94035.
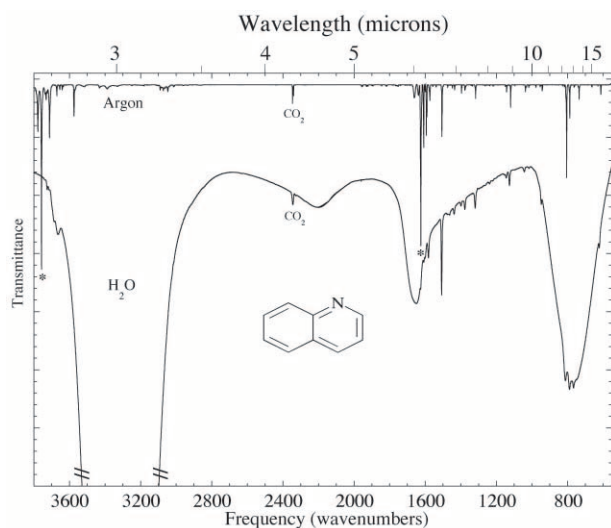[2] SETI Institute, 515 North Whisman Road, Mountain View, CA 94043.

Fig. 1.—The 3800–550 cm$^{-1}$ (2.63–18.18 $\mu$m) IR spectra of quinoline (C$_9$H$_7$N) isolated in an argon matrix (Ar/C$_9$H$_7$N > 1000; *top line*) and in solid H$_2$O (H$_2$O/C$_9$H$_7$N = 20; *bottom line*). The large broad absorptions in the (bottom) spectrum centered near 3250, 2200, 1600, and 750 cm$^{-1}$ (3.08, 4.5, 6.25, and 13.3 $\mu$m) are caused by the amorphous solid H$_2$O at 15 K. Because H$_2$O absorptions dominate the spectrum, some of the quinoline features are obscured. An asterisk below a band in the argon matrix spectrum indicates the presence of a group of peaks caused by, or with a large contribution from, matrix-isolated H$_2$O.

foot of snow on the ground in winter but very low humidity, molecules can be easily detected by IR condensed onto grains even though their gas-phase abundance is low. Moreover, IR has the advantage that it can measure absorptions of a class of molecules *summed together*, such as PAH C-H stretches (Smith et al. 1989; Sellgren et al. 1995; Brooke et al. 1999), CCC bending modes (Van Kerckhoven et al. 2000), or C-H out-of-plane bending modes (Hony et al. 2001). Thus, when the absorptions of many members of a class of molecules fall together, they can be detected, although the abundance of any one molecule is so low that it would not have been seen. In this, the first paper that presents the spectrum of PANHs under dense cloud conditions, we are starting to learn whether PANHs have absorptions that would allow us to distinguish them from those of normal PAHs in spectra of cold interstellar grains or on the surface of icy bodies in the solar system.

## 2. EXPERIMENTAL TECHNIQUES

### 2.1. Sample Preparation

The basic techniques and equipment employed for this study have been described previously as part of our previous studies of aromatics isolated in argon and in solid H$_2$O at low temperature (Mattioda et al. 2003; Sandford et al. 2004). Details associated with the materials and methods we used that are unique to this particular study are provided below.

Quinoline (98%) was purchased from the Aldrich chemical company. This amber liquid was distilled to produce a nearly colorless liquid and freeze-pump-thawed three times to remove dissolved gases. Quinoline was then sublimed from this reservoir to prepare the gas mixtures used to make our samples (see below). Phenanthridine (99+%) was purchased from Aldrich and used without further purification. The H$_2$O was purified via a Millipore Milli-Q water system to 18.2 M$\Omega$ and freeze-pump-thawed three times to remove dissolved gases prior to use. Argon (99.998%) was purchased from Matheson and used without further purification.

Quinoline had sufficient volatility at room temperature so that samples could be prepared by mixing, in the gas phase, Ar or H$_2$O vapor with quinoline vapor, as we have done with naphthalene (Sandford et al. 2004). Sample mixtures were made at room temperature in volume-calibrated, greaseless glass bulbs and allowed to equilibrate for at least 24 hr before use. The background pressure in the gas-handling system was $\sim$10$^{-6}$ mbar. The total pressure in the sample bulbs was $\sim$300 mbar for Ar mixtures and a few mbar for H$_2$O mixtures, so the contaminant levels in the bulbs associated with the mixing process were negligible compared to the original impurities of our starting materials. The Ar/quinoline ratios were in excess of 300, and H$_2$O/quinoline ratios were of 20 and 100. Thus, in argon mixtures the quinoline molecules were isolated from one another, but in the H$_2$O mixtures they were not. Therefore, the spectra of quinoline in H$_2$O may show effects from both H$_2$O-quinoline interactions and quinoline-quinoline interactions.

Once prepared, glass sample bulbs were transferred to the stainless steel vacuum manifold, where the sample mixture was vapor-deposited onto a CsI window cooled to 15 K by an Air Products Displex CSW 202 closed-cycle helium refrigerator. Our H$_2$O/quinoline mixtures were deposited first for 15 minutes against a cold shield before being deposited onto the sample window to ensure that the H$_2$O/quinoline ratio in the solid sample was representative of the gas-phase mixing ratio (i.e., 20) in the bulb. Samples were deposited at a rate sufficient to produce microns of sample on the 15 K substrate per hour. Argon samples were tens of microns, while H$_2$O samples were less than a micron thick. Under these conditions the latter samples are composed of an intimate mixture of the quinoline molecules in high-density amorphous H$_2$O. This form of H$_2$O is believed to be representative of H$_2$O-rich ices in interstellar molecular clouds (Jenniskens & Blake 1994; Jenniskens et al. 1995).

Phenanthridine samples were prepared by subliming it from a Pyrex tube at $\sim$63$^{\circ}$C directly onto the CsI substrate while codepositing either argon or H$_2$O from a room temperature bulb. As a result, we cannot know the concentration in those samples, but we estimate, based on the thickness of the argon deduced from fringes, that the phenanthridine molecules in our Ar experiments were isolated from one another, i.e., Ar/C$_{13}$H$_9$N > 300. It is much harder to tell for the corresponding H$_2$O experiments, but based on relative band areas we estimate that H$_2$O/C$_{13}$H$_9$N > 10.

### 2.2. Relative Versus Absolute Absorption Strengths

In general, we report relative areas, because we have no accurate absolute scale against which to compare the quinoline peak areas in the argon matrix. However, we can give an estimate of the intrinsic (absolute) absorptivities for quinoline in solid H$_2$O given certain assumptions. Since we know the proportions of H$_2$O and quinoline, and if we assume that the areas of H$_2$O bands in the mixture are not dissimilar to that of pure H$_2$O, then we can estimate the absolute strengths by taking the ratio of the quinoline and H$_2$O peaks (divided by the concentration). The H$_2$O-quinoline sample(s) were premixed in the gas phase at room temperature in a glass bulb at H$_2$O/C$_9$H$_7$N = 20. We estimate that the uncertainty in this measurement is *at most* 25%, and probably less. Assuming that the "*A*-values" (absolute intensities) of the H$_2$O absorptions at 3, 6.25, and 13.3 $\mu$m are $1.7 \times 10^{-16}$, $1 \times 10^{-17}$, and $2.8 \times 10^{-17}$ cm molecule$^{-1}$, respectively (Hudgins et al. 1993), this implies that the strongest peak of quinoline in H$_2$O (at 1507 cm$^{-1}$ 6.634 $\mu$m) has an *A*-value $\sim$2 $\times$ 10$^{-18}$ cm molecule$^{-1}$. Thus, the relative areas reported for C$_9$H$_7$N in H$_2$O in the far right column of Table 1 can be converted to absolute strengths, within a factor of 2 or so, by multiplying all the values by $\sim$2 $\times$ 10$^{-18}$ cm molecule$^{-1}$.

TABLE 1
Positions, Widths, and Relative Strengths of Quinoline ($C_9H_7N$)

| Matrix Isolated in Argon | | | Frozen in Solid $H_2O$ | | |
|---|---|---|---|---|---|
| Peak Position[a] [cm$^{-1}$ ($\mu$m)] | Width (cm$^{-1}$) | Area[b] | Peak Position[a] [cm$^{-1}$ ($\mu$m)] | Width (cm$^{-1}$) | Area[b] |
| 3089.9 (3.2364) | 3 | . . .[c] | | . . . | . . . |
| 3072.1 (3.2551) | 3 | . . .[c] | 3060 (3.2680) | ~30 | . . .[c] |
| 3046.6 (3.2823) | 4 | . . .[c] | | . . . | . . . |
| 3014.4 (3.3174) | 6 | . . .[c] | sh 3018 (3.3135) | ~15 | . . .[c] |
| 3117–2980 (3.208–3.356) | . . . | .95 | 3100–3000 (3.226–3.333) | . . . | $\geq$0.29[d] |
| 2961.2 (3.3770) | . . . | . . . | | . . . | . . . |
| sh 2959 (3.380) | 10 | 0.044[c] | | . . . | . . . |
| sh 2957 (3.382) | . . . | . . . | | . . . | . . . |
| sh 2954 (3.385) | . . . | . . . | | . . . | . . . |
| 2935.6 (3.4065) | 10 | 0.028 | | . . . | . . . |
| sh 1965 (5.089) | . . . | . . . | | . . . | . . . |
| sh 1962 (5.097) | . . . | . . . | | . . . | . . . |
| sh 1957 (5.110) | . . . | 0.11[c] | 1959.6 (5.1031) | ~1 | <0.01 |
| 1955.3 (5.1143) | 4 | . . . | | . . . | . . . |
| 1951.5 (5.1243) | 2 | . . . | | . . . | . . . |
| sh 1935 (5.168) | . . . | . . . | | . . . | . . . |
| 1929.7 (5.1822) | 3 | 0.11[c] | | . . . | . . . |
| sh 1927 (5.189) | . . . | . . . | | . . . | . . . |
| 1921.5 (5.2043) | 2 | . . . | | . . . | . . . |
| sh1850 (5.405) | . . . | . . . | | . . . | . . . |
| 1844.5 (5.4215) | 2 | 0.034[c] | | . . . | . . . |
| sh 1823 (5.485) | . . . | . . . | | . . . | . . . |
| 1817.6 (5.5018) | 3 | 0.05[c] | | . . . | . . . |
| sh 1815 (5.510) | . . . | . . . | | . . . | . . . |
| sh 1757 (5.692) | . . . | . . . | | . . . | . . . |
| 1751.8 (5.7084) | 2 | 0.051[c] | | . . . | . . . |
| 1720.2 (5.8133) | 7 | 0.018[c] | | . . . | . . . |
| sh 1717 (5.824) | . . . | . . . | | . . . | . . . |
| 1699.3 (5.8848) | 4 | 0.018 | | . . . | . . . |
| ~1660–1590 (6.02–6.29) | . . . | . . . | 1624.9 (6.1542) | 4 | 0.082 |
| | $H_2O$ | . . .[e] | sh 1608 (6.219) | 4 | . . . |
| | | | 1598.4 (6.2563) | 4 | 0.18 |
| sh 1577 (6.341) | . . . | . . . | | . . . | . . . |
| 1573.7 (6.3545) | 3 | 0.51 | 1581.6 (6.3227) | 7 | 0.31 |
| 1556.9 (6.4230) | 2 | 0.037 | | . . . | . . . |
| 1538.2 (6.5011) | 2 | 0.035 | | . . . | . . . |
| 1505.9 (6.6405) | 3 | 1.0 | 1507.3 (6.6344) | 5 | 1.0 |
| sh 1505 (6.645) | . . . | . . . | | . . . | . . . |
| | | | 1475.6 (6.7769) | . . . | . . . |
| 1473.5 (6.7866) | 2 | 0.035 | sh 1471 (6.798) | ~15 | 0.10 |
| | | | 1462.5 (6.8376) | . . . | . . . |
| 1461.0 (6.8446) | 1 | 0.0038 | | . . . | . . . |
| 1447.2 (6.9099) | 2 | 0.054 | | . . . | . . . |
| 1434.6 (6.9706) | 2 | 0.083 | 1437.3 (6.9575) | 6 | 0.12 |
| 1395.4 (7.1664) | 2 | 0.13 | 1398.4 (7.1510) | 6 | 0.063 |
| 1377.1 (7.2616) | . . . | . . . | | . . . | . . . |
| sh 1375 (7.273) | 4 | 0.19[c] | 1376.8 (7.2632) | 6 | 0.17 |
| 1371 (7.2945) | . . . | . . . | | . . . | . . . |
| 1334.2 (7.4951) | 1 | 0.018 | | . . . | . . . |
| sh 1319 (7.582) | . . . | . . . | 1318.8 (7.5827) | 6 | 0.28 |
| 1316.5 (7.5959) | 2 | 0.26 | | . . . | . . . |
| 1262.6 (7.9202) | 1 | 0.012 | 1258.9 (7.9434) | 8 | 0.0238 |
| 1239.6 (8.0671) | 2 | 0.0076 | 1238.3 (8.0756) | 7 | 0.041 |
| 1217.8 (8.2115) | 1 | 0.013 | 1220.3 (8.1947) | 8 | 0.021 |
| | | | ~1200 (8.333) | 10 | 0.015 |
| 1149.1 (8.7025) | 2 | 0.028 | sh 1154 (8.666) | 8 | . . . |
| 1141.9 (8.7573) | 2 | 0.11 | 1144.2 (8.7397) | . . . | 0.12 |
| 1119.7 (8.9310) | 2 | 0.28 | 1125.9 (8.8818) | 6 | 0.23 |
| 1036.3 (9.6497) | 2 | 0.17 | 1042.8 (9.5896) | 8 | 0.097 |
| sh 1032 (9.690) | . . . | . . . | | . . . | . . . |
| 1017.6 (9.8270) | 1 | 0.044 | 1016.4 (9.8386) | 5 | 0.010 |
| sh 1014 (9.862) | . . . | . . . | | . . . | . . . |

TABLE 1—*Continued*

| MATRIX ISOLATED IN ARGON | | | FROZEN IN SOLID $H_2O$ | | |
| Peak Position[a] [cm$^{-1}$ ($\mu$m)] | Width (cm$^{-1}$) | Area[b] | Peak Position[a] [cm$^{-1}$ ($\mu$m)] | Width (cm$^{-1}$) | Area[b] |
| --- | --- | --- | --- | --- | --- |
| sh 979 (10.21)............................ | ... | ... | | ... | ... |
| 976.6 (10.24)............................ | 1 | 0.044 | ~992 ........................................ | ... | <0.01 |
| sh 956 (10.46)............................ | ... | ... | | ... | ... |
| 952.8 (10.495).......................... | 2 | 0.024 | | ... | ... |
| 942.4 (10.611).......................... | 3 | 0.1 | 947.9 (10.550)........................... | 5 | 0.12 |
| sh 940 (10.64)............................ | ... | ... | | ... | ... |
| 816.8 (12.243).......................... | 1 | 0.019 | | ... | ... |
| sh 815 (12.27)............................ | ... | ... | | ... | ... |
| sh 809 (12.36)............................ | ... | ... | 812.7 (12.305).......................... | 14 | 0.84 |
| 804.0 (12.438).......................... | 2 | 1.95 | | ... | ... |
| sh 790 (12.66)............................ | ... | ... | | ... | ... |
| 786.9 (12.708).......................... | 2 | 0.52 | 789.4 (12.668).......................... | 9 | 0.27 |
| sh 783 (12.77)............................ | ... | ... | | ... | ... |
| 762.8 (13.110).......................... | 1 | 0.045 | 765.7 (13.060).......................... | 7 | 0.10 |
| sh 760 (13.16)............................ | ... | ... | | ... | ... |
| sh 738 (13.55)............................ | ... | ... | | ... | ... |
| 734.3 (13.618).......................... | 2 | 0.24 | | ... | ... |
| 612.6 (16.324).......................... | 3 | 0.16 | 620.0 (16.129).......................... | 5 | 0.15 |
| sh 611 (16.37)............................ | ... | ... | | ... | ... |

[a] Positions of "shoulders" (weak peaks on the edge of larger absorptions, marked with "sh") are given only to the nearest wavenumber, and neither areas nor widths are given for shoulders.

[b] Areas are normalized to the band near 1507 cm$^{-1}$ (6.6344 $\mu$m). These relative strengths can be converted into absolute strengths by multiplying them by a factor of ~$2 \times 10^{-18}$ cm molecule$^{-1}$ (see § 2). Peaks with areas below our threshold limit of ~1% are, in general, not included.

[c] When peaks are blended together, often only the overall area of the group is given. The positions of only the prominent peaks are given.

[d] These data were derived from a spectrum of $H_2O$/quinoline = 20 that was modified to bring out the C-H stretches (see Fig. 2, trace B), so these values should be regarded as approximate. See § 2.3 for details.

[e] The region from ~1660 to 1590 cm$^{-1}$ (6–6.3 $\mu$m) is obscured by peaks caused by $H_2O$ in the argon matrix. See Fig. 3.

### 2.3. *Uncertainties in the* C-H *Stretching Region*

The positions, widths, and relative areas reported for quinoline C-H stretching features (in the 3.2–3.4 $\mu$m region) should be regarded as more uncertain than the other quinoline absorptions. This uncertainty results primarily from the proximity to the very strong 3 $\mu$m $H_2O$ band. The values reported in the tables for the C-H stretches of both quinoline and phenanthridine were derived from spectra that had been modified to remove the strong $H_2O$ band that masked the quinoline absorptions (compare traces A and B in Fig. 2, for an example). This was done in the following manner: an IR spectrum of pure $H_2O$ was measured under conditions identical to those of the $H_2O$/PANH mixtures, and it was scaled so that the 3 $\mu$m $H_2O$ band in the spectra matched. Then, the spectrum of pure $H_2O$ was gradually subtracted from the spectrum of the $H_2O$/PANH mixture until the C-H stretching features were revealed. Naturally, the spectrum of pure $H_2O$ is not identical to that of $H_2O$ in mixture, so attempting to subtract out all of the $H_2O$ absorptions resulted in artifacts (such as negative peaks in some regions). We found that removing ~75% of the $H_2O$ gave a spectrum in which the quinoline C-H absorptions were apparent, while the spectrum seemed free of obvious aberrations, and this is what appears in Figure 2. Similarly, removal of ~70% of $H_2O$ from the spectrum of the $H_2O$ phenanthridine mixture was used to determine the phenanthridine C-H stretching values that appear in Table 2.

The C-H stretching features are certainly more prominent in the spectra that result from the subtraction of pure $H_2O$ than in the originals, but even so there is some ambiguity in the positions and widths of these peaks. Just as with astronomical spectra, one has to assume a certain baseline, and in the case of the

$H_2O$-quinoline mixture we felt that the most reasonable approach was to assume a flat "baseline" from 3.231 to 3.339 $\mu$m (3095–2995 cm$^{-1}$). This results in two broad blended features: a larger, shorter wavelength one centered at ~3.268 $\mu$m (3060 cm$^{-1}$) with a full width at half-height of ~0.064 $\mu$m (30 cm$^{-1}$) and another smaller one centered at 3.3135 $\mu$m (3018 cm$^{-1}$) that is approximately 0.033 $\mu$m (15 cm$^{-1}$) wide (see Table 1). See § 4.1 for the influence this choice may have on the apparent peak positions and widths.

Finally, the proximity of our laboratory to San Francisco Bay marshlands caused some methane contamination in our purge gas, so weak features of gas-phase $CH_4$ also had to be removed from this region of the spectrum of quinoline in $H_2O$. This final correction probably did not have any effect on the values reported in the tables.

### 3. RESULTS

Selected portions of the IR spectrum of the two-ring PANH quinoline (and many other PANHs) in an inert matrix have been published previously (Garrison et al. 1982), but this represents the first presentation of the full mid-IR spectrum of quinoline and phenanthridine in an argon matrix and in solid $H_2O$. In the following sections we report and compare the spectral properties (band positions, widths, and relative strengths) of $C_9H_7N$ and $C_{13}H_9N$ in an Ar matrix and $H_2O$.

### 3.1. *IR Spectra of Quinoline* ($C_9H_7N$)

The 3800–550 cm$^{-1}$ (2.63–18.18 $\mu$m) IR spectra of quinoline ($C_9H_7N$) isolated in an argon matrix (Ar/$C_9H_7N$ > 1000) and in solid $H_2O$ ($H_2O$/$C_9H_7N$ ≈ 20) are presented in Figure 1. The large broad absorptions in the latter (*bottom spectrum*)
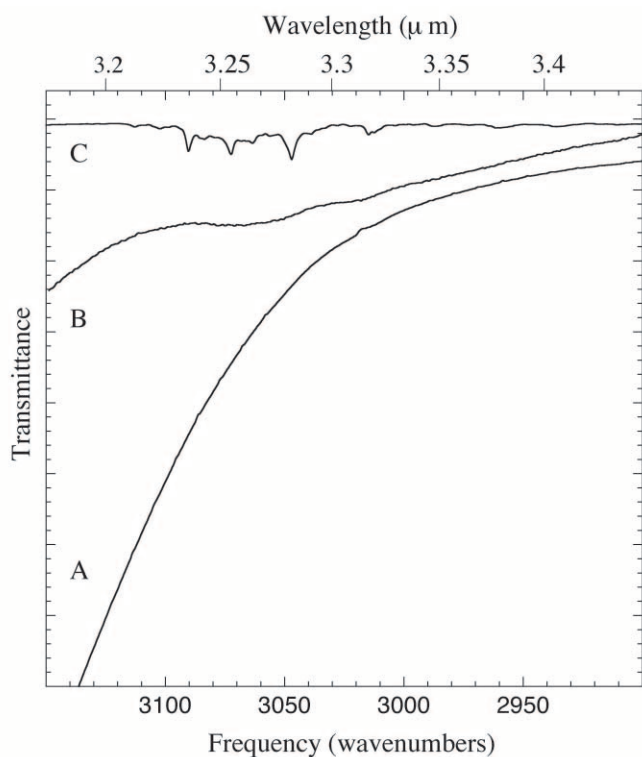
FIG. 2.—The 3150–2900 cm$^{-1}$ (3.175–3.448 $\mu$m) IR spectra, from bottom to top, of quinoline in solid H$_2$O at 15 K (H$_2$O/C$_9$H$_7$N $\approx$ 20; *trace A*) quinoline in H$_2$O *minus* 75% of a comparable spectrum of pure H$_2$O (*trace B*), and quinoline isolated in an argon matrix (Ar/C$_9$H$_7$N > 1000; *trace C*) at 15 K. Although the weak aromatic C-H absorptions in trace A are obscured by the long-wavelength wing of the 3 $\mu$m H$_2$O, the partial subtraction of pure H$_2$O reveals the C-H stretches of quinoline in H$_2$O as broad absorptions in trace B spanning the range from ~3090 to ~3025 cm$^{-1}$ (3.24–3.3 $\mu$m), as opposed to the distinct sharp absorptions of quinoline isolated in argon (*trace C*). Such broad absorptions are to be expected, since H$_2$O tends to interact strongly with neighboring molecules. The position and width of these broad features of quinoline in H$_2$O are discussed in the context of astronomical observations of aromatic absorptions in § 4.1.

centered near 3250, 2200, 1600, and 750 cm$^{-1}$ (3.08, 4.5, 6.25, and 13.3 $\mu$m) are caused by the amorphous solid H$_2$O at 15 K. Table 1 lists the peak positions, FWHMs, and relative areas of the strongest quinoline bands for both argon and solid H$_2$O matrices.

Expansions of these spectra in the 3150–2900 cm$^{-1}$ (3.175–3.448 $\mu$m) region are presented in Figure 2. The strong 3250 cm$^{-1}$ (3.08 $\mu$m) H$_2$O peak makes it very difficult to discern the quinoline C-H stretches that are plainly evident in the spectrum of quinoline in argon (compare traces A and C in Fig. 2). This is very similar to what we observed in the laboratory spectra of naphthalene in solid H$_2$O (Sandford et al. 2004). Such weak aromatic C-H absorptions on the wing of the 3 $\mu$m H$_2$O band are very subtle, and yet they have been observed at 3.25 $\mu$m (~3077 cm$^{-1}$) toward Mon R2 IRS 3 (Sellgren et al. 1995), S140 IRS 1 and NGC 7538 IRS 1 (Brooke et al. 1996), and Ser SVS 20 and R CrA IRS 1 (Brooke et al. 1999).

These C-H stretching features can be made more obvious in the laboratory data by partial spectral subtraction of a laboratory spectrum of pure H$_2$O under identical conditions. The resulting spectrum of quinoline in H$_2$O from which some pure H$_2$O has been subtracted (Fig. 2, *trace B*) reveals that the C-H stretches of quinoline in H$_2$O are present as two broad absorptions spanning the range from ~3090 to ~3000 cm$^{-1}$ (3.24–3.33 $\mu$m), as opposed to the many distinct sharp absorptions of quinoline iso-

lated in argon (Fig. 2, *trace C*). The fact that these features are sharp and distinct in the spectrum of quinoline in the argon matrix but are broad and overlapping in solid H$_2$O is to be expected, since H$_2$O tends to interact strongly with neighboring molecules, whereas argon is inert and thus chosen for matrix isolation studies intended to mimic the gas phase (Allamandola et al. 1999).

The overall range spanned by this broad ensemble of overlapping C-H peaks in the H$_2$O-quinoline mixture corresponds roughly to the range in which these features fall in the spectrum of matrix-isolated quinoline (compare the downward absorptions in traces B and C in Fig. 2). Thus, while the C-H stretching absorptions of quinoline in H$_2$O are broader, they have not shifted significantly (relative to their width) compared to those of quinoline in argon. The broadening of the aromatic C-H stretches with little variation in position is similar to our results for naphthalene in H$_2$O (Sandford et al. 2004). On the whole, the position and width of the aromatic C-H stretches of quinoline in H$_2$O are generally consistent with astronomical observations of aromatic C-H stretches in absorption (Sellgren et al. 1995; Brooke et al. 1996, 1999; Chiar et al. 2000), and a closer analysis including comparisons to astronomical observations appears in § 4.1.

The C-H stretches are not the only quinoline absorptions that are broader in the presence of H$_2$O than in the spectrum of quinoline isolated in argon. As we saw for naphthalene in H$_2$O, and as we see below at longer wavelengths, interactions with H$_2$O cause all of the quinoline absorptions to be broader. Moreover, at longer wavelengths we note clear shifts in position as well.

The IR spectra of molecules in argon matrices are frequently complicated by the presence of small amounts of matrix-isolated H$_2$O, a common contaminant that, in this case, is probably derived from H$_2$O dissolved in the original quinoline sample. The matrix is so dilute that the H$_2$O molecules are probably not interacting directly with the quinoline molecules, but they contribute to the ensemble of peaks in the 1600 cm$^{-1}$ (6.25 $\mu$m) region of the Ar spectrum in Figure 3. This makes it difficult to distinguish what peaks in this region are caused by quinoline. This problem is mitigated in the corresponding spectrum of quinoline in H$_2$O, because all of the sharp H$_2$O peaks have been converted to the broad underlying 6.25 $\mu$m absorption, revealing the quinoline peaks as shoulders between 1630 and 1570 cm$^{-1}$ (6.14–6.37 $\mu$m). Theoretical calculations (D. E. Woon et al. 2005, in preparation) and spectra of neat (room temperature) quinoline indicate that there should be three quinoline peaks in this region near 1620, 1596, and 1570 cm$^{-1}$ (6.17, 6.27, and 6.37 $\mu$m).

Figure 4 displays the 1490–900 cm$^{-1}$ (6.71–11.11 $\mu$m) spectral region, where quinoline peaks suffer from the least interference from H$_2$O absorption bands. This region contains some of the peaks that show the largest shifts between the matrices of argon and solid H$_2$O. Many of the sharp peaks of quinoline in argon became broader and moved to higher frequency as a result of interactions with H$_2$O. For example, of the 10 peaks marked with dashed lines in Figure 4, nine of them appear at higher frequency in the lower spectrum; only that at 1377 cm$^{-1}$ (7.62 $\mu$m) appears not to have done so, perhaps because of blending with lower frequency shoulders. This tendency of quinoline peaks to appear at higher frequency in solid H$_2$O than in argon matrix is also seen for absorption bands in the C-H out-of-plane region (Fig. 5) and is consistent with the previously reported interaction of pyridine and pyrimidine with H$_2$O in Ar matrices (Destexhe et al. 1994).

TABLE 2
POSITIONS, WIDTHS, AND RELATIVE STRENGTHS OF PHENANTHRIDINE

| | MATRIX ISOLATED IN ARGON | | | FROZEN IN SOLID $H_2O$ | |
|---|---|---|---|---|---|
| Peak Position[a] [cm$^{-1}$ ($\mu$m)] | Width (cm$^{-1}$) | Area[b] | Peak Position[a] [cm$^{-1}$ ($\mu$m)] | Width (cm$^{-1}$) | Area[b] |
| 3114.8 (3.2105) | 10 | . . .[c] | | . . . | . . . |
| 3078.7 (3.2481) | 30 | . . .[c] | | . . . | . . . |
| 3044.5 (3.2846) | 6 | . . .[c] | | . . . | . . . |
| 3034.3 (3.2846) | 6 | . . .[c] | | . . . | . . . |
| 3120–3000 (3.205–3.333) | . . .[c] | 0.77 | 3069 (3.258) | ~60 | 1.0[d] |
| 2966.3 (3.3712) | 20 | . . .[c] | | . . . | . . . |
| 2993.9–2916.8 (3.3401–3.4284) | . . .[c] | 0.22 | | . . . | . . . |
| sh 1961 (5.099) | . . . | . . . | | . . . | . . . |
| 1957.1 (5.1096) | 6 | 0.051 | | . . . | . . . |
| sh 1953 (5.120) | . . . | . . . | | . . . | . . . |
| 1937 (5.163) | . . . | . . . | | . . . | . . . |
| 1924 (5.198) | 3–4 | 0.059[c] | | . . . | . . . |
| 1916 (5.219) | . . . | . . . | | . . . | . . . |
| 1908 (5.241) | . . . | . . . | | . . . | . . . |
| 1835.3 (5.449) | 5 | 0.016 | | . . . | . . . |
| 1822 (5.489) | . . . | . . . | | . . . | . . . |
| 1814 (5.513) | 2–3 | 0.016[c] | | . . . | . . . |
| 1807 (5.534) | . . . | . . . | | . . . | . . . |
| | . . . | . . . | 1623.8 (6.1584) | 6 | 0.26 |
| ~1660–1590 (6.02–6.29) | . . . | . . .[e] | sh 1615 (6.192) | . . . | . . . |
| | . . . | . . . | sh 1593 (6.278) | . . . | . . . |
| | . . . | . . . | 1582.0 (6.3211) | 5 | 0.16 |
| sh 1533 (6.522) | . . . | . . . | | . . . | . . . |
| 1530.1 (6.5355) | 2 | 0.083 | 1529.9 (6.5364) | 7 | 0.13 |
| sh 1496 (6.685) | . . . | . . . | | . . . | . . . |
| 1492.7 (6.6993) | 2 | 0.20 | 1494.6 (6.6908) | 8 | 0.16 |
| 1463.2 (6.8343) | 3 | . . . | 1461.5 (6.8423) | 7 | . . . |
| sh 1453 (6.882) | . . . | 0.19 | | . . . | 0.40 |
| 1449.3 (6.8999) | 3 | . . . | 1448.7 (6.9027) | 6 | . . . |
| 1418.2 (7.0512) | 3 | 0.013 | 1418.7 (7.0487) | 6 | 0.016 |
| 1397.3 (7.1567) | 4 | . . .[b] | 1398.2 (7.1521) | 13 | 0.039 |
| 1343.5 (7.4432) | . . . | . . . | | . . . | . . . |
| 1339.7 (7.4644) | 6 | 0.060[c] | 1344.4 (7.4383) | 12 | 0.12 |
| 1334.7 (7.4923) | . . . | . . . | | . . . | . . . |
| 1295.9 (7.7166) | 2 | 0.026 | 1297.4 (7.7077) | 17 | 0.027 |
| | . . . | . . . | sh 1285 (7.782) | . . . | . . . |
| sh 1244 (8.039) | . . . | . . . | 1244.3 (8.0366) | 8 | 0.26 |
| 1240.8 (8.0593) | 4 | 0.24 | sh 1232 (8.117) | . . . | . . . |
| 1194.7 (8.3703) | 3 | 0.028 | 1197.0 (8.3542) | 8 | 0.019 |
| 1164.8 (8.5852) | 2 | 0.013 | 1166.9 (8.5697) | 7 | 0.012 |
| 1149.7 (8.6979) | 1 | 0.0092 | sh 1150 (8.696) | 6 | 0.084 |
| 1145.3 (8.7313) | 3 | 0.028 | 1141.2 (8.7627) | . . . | . . . |
| 1137.4 (8.7920) | 3 | 0.037 | | . . . | . . . |
| 1101.3 (9.0802) | 2 | 0.0043 | 1103.4 (9.0629) | 5 | 0.011 |
| 1041.8 (9.5988) | 1 | . . . | | . . . | . . . |
| 1038.5 (9.6293) | 3 | 0.030 | 1034.0 (9.6712) | 7 | 0.031 |
| sh 1035 (9.662) | . . . | . . . | | . . . | . . . |
| 1005.2 (9.9483) | 2 | 0.018 | 1004.4 (9.9562) | 3 | 0.0047 |
| sh 960 (10.417) | . . . | 0.071 | | . . . | . . . |
| 958.1 (10.437) | 1 | . . . | ~967 (10.34) | ~9 | 0.014 |
| 930.7 (10.745) | 2 | 0.038 | | . . . | . . . |
| 899.1 (11.122) | 1 | 0.0033 | | . . . | . . . |
| 892.7 (11.202) | 1 | 0.14 | ~897 (11.15) | ~9 | 0.097 |
| 889.7 (11.240) | 4 | . . . | | . . . | . . . |
| | . . . | . . . | ~834 (11.99) | ~6 | 0.013 |
| 793.0 (12.610) | 2 | 0.013 | ~796 (12.56) | ~6 | 0.020 |
| 767.2 (13.034) | 2 | 0.12 | ~778 (12.85) | ~8 | 0.015 |
| 747.3 (13.382) | 3 | 1.0 | 752.5 (13.29) | ~17 | 1.0 |

TABLE 2—*Continued*

| Matrix Isolated in Argon | | | Frozen in Solid H$_2$O | | |
|---|---|---|---|---|---|
| Peak Position[a] [cm$^{-1}$ ($\mu$m)] | Width (cm$^{-1}$) | Area[b] | Peak Position[a] [cm$^{-1}$ ($\mu$m)] | Width (cm$^{-1}$) | Area[b] |
| 729.7 (13.704)........................... | 1 | 0.054 | | ... | ... |
| 727.2 (13.751)........................... | 2 | ... | | ... | ... |
| 720.6 (13.877)........................... | 1 | 0.11 | 720.7 (13.875)........................... | ~6 | 0.15 |
| ... | ... | ... | sh 713 (14.03)....................... | ... | ... |
| 615.4 (16.250)........................... | 1 | 0.068 | ~614 (16.29) ........................... | ~3 | 0.039 |

[a] Positions of "shoulders" (weak peaks on the edge of larger absorptions, marked with "sh") are given only to the nearest wavenumber, and neither areas nor widths are given for shoulders.

[b] Areas are listed only for the larger peaks; those below our threshold limit of ~2% relative to the strongest absorption could not be integrated accurately. Areas are normalized to the peak near 750 cm$^{-1}$ (13.3 $\mu$m).

[c] When peaks are blended together, often only the overall area of the group is given. The positions of only the largest peaks are given.

[d] These data were derived from a spectrum that was modified to bring out the C-H stretches (see § 2.3 for details), so these values should be regarded as approximate.

[e] The region from ~1660 to 1590 cm$^{-1}$ (6.0–6.3 $\mu$m) is obscured by peaks caused by H$_2$O in the argon matrix.

In most cases the new positions of the peaks of quinoline in solid H$_2$O are easy to discern, but sometimes the shifts are sufficiently large that it is difficult to determine where peaks have moved. For example, in Figure 4 the sharp peak in the upper spectrum near 1445 cm$^{-1}$ (6.92 $\mu$m) has presumably become part of the complex of broad overlapping peaks between 1460 and 1480 cm$^{-1}$ in the lower spectrum (see arrow in Fig. 4). Similar changes in position and relative area occur in the smaller peaks between 1200 and 1225 cm$^{-1}$ (8.33–8.16 $\mu$m). Other quinoline peaks, such as the one near 976 cm$^{-1}$ (10.25 $\mu$m) in argon, are almost lost because they fall on the edge of a strong H$_2$O feature. Like the C-H stretches in Figure 2, this absorption is, in fact, still present in the lower spectrum at ~992 cm$^{-1}$ (10.08 $\mu$m), but it is difficult to discern because of the nearby 750 cm$^{-1}$ (13.3 $\mu$m) H$_2$O feature.

The quinoline peak at 734 cm$^{-1}$ (13.62 $\mu$m) in Figure 5 is quite obvious in the argon spectrum, but hard to perceive in the lower H$_2$O spectrum. There is perhaps a hint of a band near ~740 cm$^{-1}$ (13.51 $\mu$m), but it is unclear why this one would be so affected when the others are less so. Perhaps the area of this 734 cm$^{-1}$ peak has been suppressed or it has broadened considerably in the presence of H$_2$O. However, it would have to be a change of *at least* a factor of 10 in relative area or width given that the absorption at 734 cm$^{-1}$ (13.62 $\mu$m) is 5 times more intense than that at 763 cm$^{-1}$ in argon, whereas in the H$_2$O spectrum if there were a peak with half the area of that at 763 cm$^{-1}$, it would presumably be evident. It is to be hoped that future chemical modeling will help to solve this mystery (D. E. Woon et al. 2005, in preparation).

### 3.2. *Changes in Relative and an Estimate of Absolute Areas*

A summary of the relative intensities of the quinoline bands can be found in Table 1. These are merely relative, because we
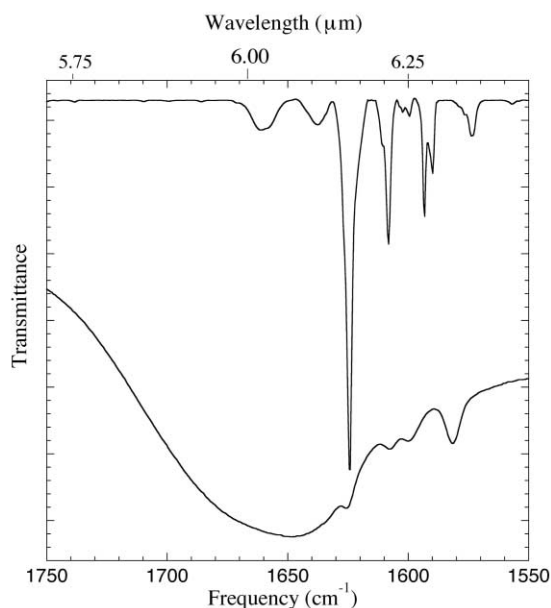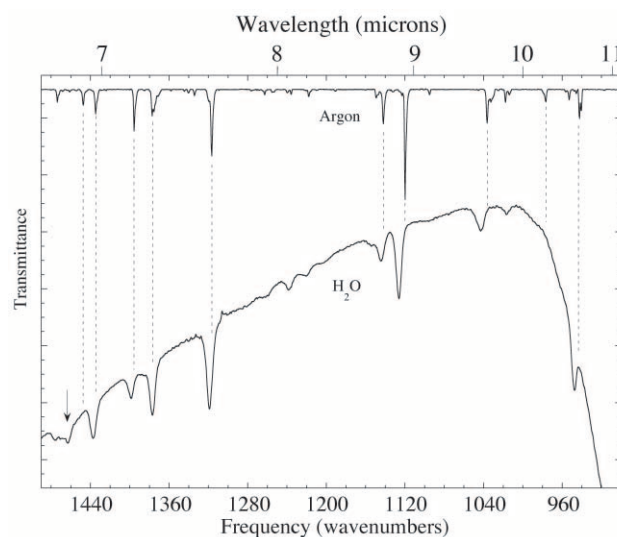


Fig. 3.—The 1750–1550 cm$^{-1}$ (5.71–6.45 $\mu$m) IR spectra of quinoline isolated in an argon matrix (Ar/C$_9$H$_7$N > 1000; *top line*) and in solid H$_2$O (H$_2$O/C$_9$H$_7$N ≈ 20; *bottom line*) at 15 K. The ensemble of peaks in the top spectrum contains major contributions from matrix-isolated H$_2$O, making it unclear whether any quinoline peaks are present. However, in the bottom spectrum the H$_2$O has blended into the broad underlying absorption feature, revealing quinoline peaks as shoulders between 1630 and 1570 cm$^{-1}$ (6.14–6.37 $\mu$m).



Fig. 4.—The 1490–900 cm$^{-1}$ (6.71– 11.1 $\mu$m) IR spectra of quinoline isolated in an argon matrix (Ar/C$_9$H$_7$N > 1000; *top line*) and in solid H$_2$O (H$_2$O/C$_9$H$_7$N = 20; *bottom line*) at 15 K. The vertical dashed lines help to show that the positions of many of the peaks of quinoline in H$_2$O are shifted to higher frequency relative to those in the Ar matrix. An arrow indicates the most extreme example of this, a feature in H$_2$O that presumably corresponds to the peak near 1445 cm$^{-1}$ (6.92 $\mu$m) in the argon spectrum.
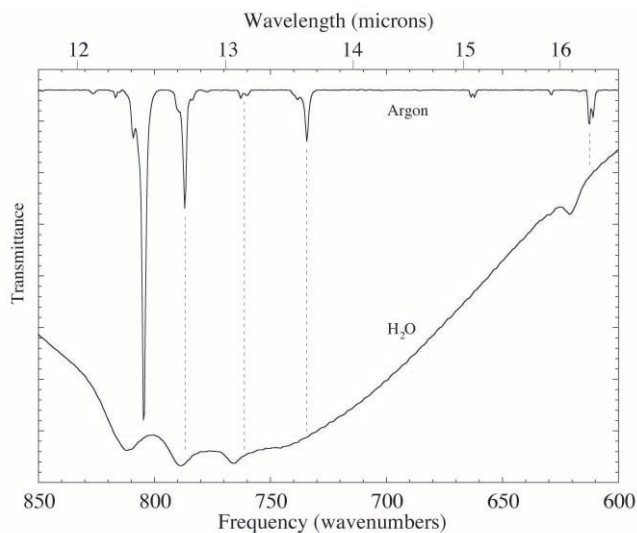
FIG. 5.—The 850–600 cm$^{-1}$ (11.76–16.67 $\mu$m) IR spectra of quinoline isolated in an argon matrix (Ar/C$_9$H$_7$N > 1000; *top line*) and in solid H$_2$O (H$_2$O/C$_9$H$_7$N = 20; *bottom line*) at 15 K. The vertical dashed lines highlight shifts to higher frequency in the positions of absorptions corresponding to C-H out-of-plane bending motions of quinoline in the presence of H$_2$O.



FIG. 6.—The 840–740 cm$^{-1}$ (11.9–13.5 $\mu$m) IR spectrum of quinoline in solid H$_2$O (H$_2$O/C$_9$H$_7$N ≈ 20) at six temperatures between 15 and 125 K. The positions of the C-H out-of-plane bending motions of quinoline depend slightly on temperature over this >100 K range.

have no absolute scale against which to compare the quinoline intensities in argon matrix. However, we have estimated rough absolute values for quinoline in solid H$_2$O given certain assumptions (see § 2). The relative strengths reported for C$_9$H$_7$N in H$_2$O in the right column of Table 1 can be converted to absolute strengths, within a factor of 2 or so, by multiplying all the values by ∼2 × 10$^{-18}$ cm molecule$^{-1}$.

A number of significant changes in the relative intensities of various quinoline bands occur between the two matrices. For example, in the spectrum of argon matrix–isolated quinoline there is an intense band at 804 cm$^{-1}$ (12.438 $\mu$m) with a shoulder at 809 cm$^{-1}$ (12.36 $\mu$m) having a relative area of almost 2 (relative to 1507 cm$^{-1}$ peak; see Table 1). The matching absorption in the H$_2$O spectrum near 813 cm$^{-1}$ (12.3 $\mu$m) has a relative area of 0.84, corresponding to a factor of 2.3 decrease in area. This was surprising, because one might expect the absorption in the H$_2$O spectrum, if anything, to be larger, since it should also include the area of nearby small peaks that are separate in the argon spectrum. Similarly, the peaks near 790 cm$^{-1}$ (12.66 $\mu$m) are almost twice as intense in argon as in H$_2$O. However, the absorptions in the spectrum of matrix-isolated quinoline are not always more intense than the equivalent one in H$_2$O. The quinoline peak near 765 cm$^{-1}$ (13.1 $\mu$m) reverses the trend, being more than twice as intense in the spectrum of the H$_2$O quinoline mixture. These serve to illustrate that quinoline features not only change position but also intrinsic strength on going from an argon matrix to solid H$_2$O at 15 K.

### 3.3. The Effects of Temperature on the Spectra of Quinoline (C$_9$H$_7$N)-H$_2$O

Examples of the modest effects of warming on the positions of quinoline absorptions in the H$_2$O/(C$_9$H$_7$N) = 20 mixture are shown in Figure 6. Warming of the sample from 15 to 125 K causes changes of only 3–4 cm$^{-1}$ in the positions of the quinoline C-H out-of-plane bending mode peaks near 800 cm$^{-1}$ (12.5 $\mu$m), and this is typical of the shifts seen elsewhere in the spectra. The absence of dramatic effects of temperature below 125 K is consistent with our previously reported observations of naphthalene (Sandford et al. 2004).
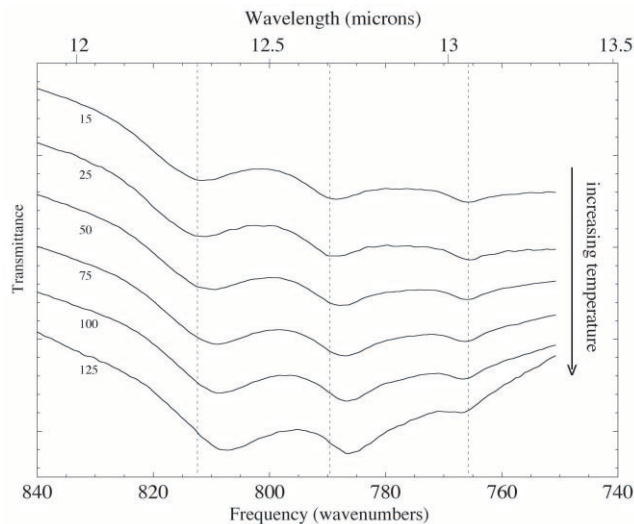
### 3.4. The Infrared Spectrum of Phenanthridine (C$_{13}$H$_9$N)

Unlike quinoline, the positions of IR absorptions of phenanthridine in H$_2$O are very similar to that of matrix-isolated phenanthridine. This is illustrated by the comparison shown in Figure 7 and the values reported in Table 2. Other than the peak broadening that commonly accompanies condensing an aromatic hydrocarbon with H$_2$O, the appearances of the spectra are remarkably similar. These IR spectra suggest that despite the presence of a nitrogen atom, there is no indication that phenanthridine is interacting with the H$_2$O molecules any more than naphthalene (Sandford et al. 2004) or the other plain PAHs (Bernstein et al. 2005).



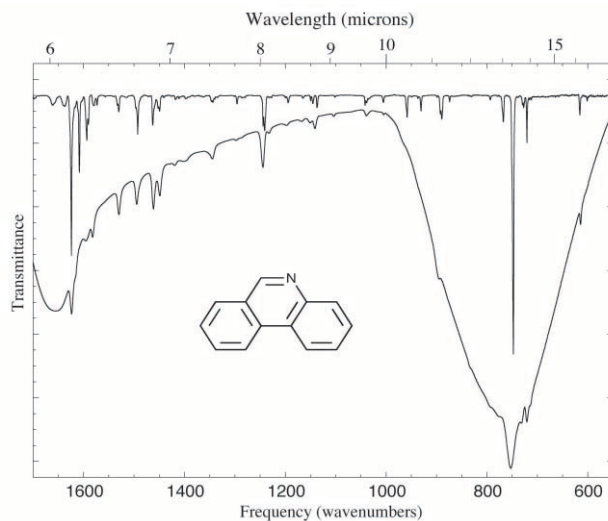FIG. 7.—The 1700–550 cm$^{-1}$ (5.88–18 $\mu$m) IR spectra of phenanthridine (C$_{13}$H$_9$N) isolated in an argon matrix (Ar/C$_{13}$H$_9$N > 1000; *top line*) and in solid H$_2$O (H$_2$O/C$_9$H$_7$N > 10; *bottom line*). The large broad absorptions in the (bottom) spectrum centered near 1600 and 750 cm$^{-1}$ (6.25 and 13.3 $\mu$m) are caused by the amorphous solid H$_2$O at 15 K. The positions of the phenanthridine peaks are essentially unchanged. As was the case with the spectrum of matrix-isolated quinoline (Fig. 3), the ensemble of peaks near the 1600 cm$^{-1}$ (6.25 $\mu$m) region of the top spectrum contain significant contributions from matrix-isolated H$_2$O.

## 4. IMPLICATIONS

The laboratory results presented here have a number of implications for the detection and identification of PANHs in absorption in interstellar dense molecular clouds. In general, PANHs are like PAHs in the intensity of the absorptions ($10^{-18}$ cm molecule$^{-1}$) and thus the limits of their detection by IR astronomy. Could such molecules ever be detected? If, consistent with aromatics in primitive meteorites, we assume there is one nitrogen atom for every hundred carbon atoms in interstellar aromatic material, then there would be roughly one quinoline for every ten naphthalenes. In such a ten-to-one mix the quinoline would be easily discernible from naphthalene. This is a very simple-minded analysis, of course, and the interstellar molecules are probably larger, but these are the spectra that we have at the moment, so we make the comparison of the molecules studied here and their PAH counterparts in hopes that they are representative of the class. Nevertheless, given that most PANHs seem to have a stronger absorption in the 6.6 $\mu$m region than normal PAHs, it seems reasonable that they contribute a measurable part of the "unidentified infrared" (UIR) emission there (Mattioda et al. 2003).

### 4.1. *Detection of PANHs in Astrophysical Ices*

In dense clouds in which other ice components obscure PAH absorptions, quinoline or any other PANH would be hard to detect. But perhaps with very good signal-to-noise ratios around 6.6 $\mu$m, where all PANHs have very strong absorptions, one might, toward a line of sight where strong PAH absorptions have been observed, be able to detect a feature a factor of 2–10 weaker than the corresponding normal PAH features.

Intermolecular interactions between quinoline and $H_2O$ lead to significant differences between the IR spectra of quinoline in an argon matrix and in solid $H_2O$ at 15 K. Thus, in contrast to normal PAHs, the peak positions and strengths of PANHs in inert gas matrices and/or measured or calculated gas-phase PANHs cannot always be relied upon to very accurately predict the positions and strengths of absorption features of PANHs in dense clouds.

Since most aromatic C-H stretches fall at the same characteristic wavelengths (3.25–3.3 $\mu$m), they remain a secure representative of the class, and their overlap permits detection of the class at a lower concentration than would be possible for any individual aromatic molecule. However, their usefulness may also be mitigated by their very poor spectral contrast in $H_2O$-rich ices because of their proximity to the very strong 3.08 $\mu$m $H_2O$ band. In addition, the lack of variation in position of aromatic C-H stretches would seem to limit their power to discriminate between different types of aromatics. Nevertheless, it is interesting to note that there is a difference in the position of the aromatic C-H stretches between young stellar objects (YSOs), where it is consistently 3.25 $\mu$m (Brooke et al. 1999), and a Galactic center line of sight (GCS 3), where it was 3.28 $\mu$m (Chiar et al. 2000).

Before attempting to compare those astronomical observations in the C-H stretching region to our laboratory data, we must review the special factors that may limit our accuracy in this region. First, the weak aromatic stretches of quinoline in $H_2O$ were obscured by the long-wavelength wing of the 3 $\mu$m $H_2O$ and were exposed by the partial subtraction of a spectrum of pure $H_2O$ (see § 2.3). Second, just as with astronomical spectra, one has to assume a certain baseline, and to some extent this determines the apparent center of the absorption. Both of these add to the uncertainty of the values associated with the C-H stretches, but we shall discuss this latter cause of error in greater detail because it determines whether the laboratory spectrum in the 3.3 $\mu$m region looks more like a YSO or a Galactic center line of sight.

In the case of the $H_2O$-quinoline mixture illustrated in Figure 2, we felt that the most reasonable approach was to assume a flat baseline in trace B from 3.231 to 3.339 $\mu$m (3095–2995 cm$^{-1}$). This resulted in two broad blended features: a larger, shorter wavelength one centered at $\sim$3.268 $\mu$m (3060 cm$^{-1}$) with a FWHM of $\sim$0.064 $\mu$m (30 cm$^{-1}$) and another smaller one centered at 3.3135 $\mu$m (3018 cm$^{-1}$) with a FWHM of $\sim$0.033 $\mu$m (15 cm$^{-1}$). These subfeatures are visible in the laboratory data because of our high signal-to-noise ratio, but such a double-peaked structure might simply appear as a single broad asymmetric feature in an astronomical spectrum. If that were the case, then the C-H stretches would probably appear to be centered at $\sim$3.284 $\mu$m ($\sim$3045 cm$^{-1}$) with a FWHM of 0.14 $\mu$m (65 cm$^{-1}$). If one drew a baseline beneath the stronger, shorter wavelength peak alone, from 3.231 to 3.300 $\mu$m (3095–3030 cm$^{-1}$), ignoring the longer wavelength feature, one would get a single peak centered at $\sim$3.263 $\mu$m (3065 cm$^{-1}$) with a FWHM of $\sim$0.064 $\mu$m (30 cm$^{-1}$).

If the C-H stretches of quinoline in $H_2O$ appeared in an astronomical spectrum blended together as a single broad feature, it would be centered at $\sim$3.28 $\mu$m, essentially the same position as that observed by Chiar et al. (2000) toward GCS 3, but with a FWHM twice that of the astronomical absorption. On the other hand, if the stronger, shorter wavelength feature is considered separately, its center is very close ($\sim$0.01 $\mu$m) to those of YSOs (Brooke et al. 1999). The FWHM of this shorter wavelength feature in the laboratory spectrum is approximately half that of the absorption toward YSOs, but this is not inconsistent with molecules of this class contributing to the observed absorptions. As for the single broad 3.26 $\mu$m phenanthridine C-H absorption, it more closely resembles YSOs than the Galactic center, both in position and FWHM. It is important to recall that astronomical observations sample a distribution of molecules, so the 3.25 $\mu$m YSO absorptions, for example, must be a combination of overlying aromatic C-H stretches with slightly different positions that all together make up that $\sim$75 cm$^{-1}$ wide absorption. The majority of this feature is probably caused by normal PAHs, and only part (perhaps 10% if meteorites are indicative) is contributed by PANHs such as quinoline and phenanthridine.

The longer wavelength IR absorption bands of quinoline (Figs. 4 and 5) show a stronger dependence than the (shorter wavelength) C-H stretches (Fig. 2). Thus, the longer wavelength absorptions of quinoline, the ones that are most indicative of a nitrogen in the ring, are also the most affected by intermolecular interactions.

In contrast to quinoline, there are no significant differences in the positions of the peaks in the IR spectra of phenanthridine in solid $H_2O$ and in an argon matrix. This, despite the fact that phenanthridine possesses a nitrogen atom that should be just as accessible to surrounding $H_2O$ molecules as that of quinoline. Thus, the presence of a nitrogen atom in an aromatic may result in a sensitivity of the IR spectrum to matrix effects, but there is no guarantee that it will.

The large variations seen for quinoline, accompanied by the relative small changes seen for phenanthridine, suggest that the presence of a nitrogen atom in PANHs can have a major effect on their interaction with $H_2O$-rich matrices, but that this interaction must be very sensitive to the geometry and placement of the N atom. Thus, in contrast to the case for PAHs, it is less safe

to predict the general spectral characteristics of PANHs in $H_2O$ based on their spectra from argon matrix isolation experiments.

These contrasting results between quinoline and phenanthridine suggest that for this class of aromatics bearing nitrogen atoms we currently lack a reliable method for predicting the precise positions of IR absorptions in interstellar dense clouds short of measuring the spectra of each molecule in solid $H_2O$. Uncertainties in the effects of $H_2O$ on the intrinsic absorptivities ($A$-values) mean that similar problems exist with the estimation of column densities of any PANHs in dense clouds one might manage to identify. It is to be hoped that a better understanding of the intermolecular interactions that govern the appearance of the IR spectra will free the community from the slow and onerous task of measuring these molecules individually in $H_2O$.

### 4.2. Astrobiology of PANHs

There are few papers that present laboratory spectra of polycyclic aromatic nitrogen heterocycles under conditions germane to astrophysics (Mattioda et al. 2003), nor have they been the subject of many interstellar searches (Kuan et al. 2003). However, these compounds, including the two molecules studied in this paper, have been extracted from carbonaceous chondrites such as the Murchison and Tagish Lake meteorites (Stoks & Schwartz 1982; Pizzarello 2001), and their aromatic structure is consistent with those that are expected to form and survive in space and in planetary atmospheres (Ricca et al. 2001).

Moreover, it is difficult to imagine a class of compounds more fundamental to biochemistry than nitrogen heterocycles. For example, purines and pyrimidines (the informational elements of DNA and RNA, which have been found in carbonaceous chondrites), two amino acids, and numerous other vital bioorganic compounds (such as flavins, porphrins, and nicotinamides) central to informational and metabolic systems are single and fused rings of carbon atoms containing nitrogen atoms. The fundamental nature of nitrogen heterocycles to terrestrial biology suggests that they should be considered as potentially astrobiologically important compounds for two reasons. First, as evidenced by their presence in meteorites, they must have been exogenously delivered to the early Earth and thus may have played a role in the origin or evolution of our biochemistry. Second, the presence of this class of molecules, which includes nucleobases, porphrins, and flavins, could act as false biomarkers, confusing the search for compounds that indicate signs of life in the universe.

### 5. CONCLUSIONS

We have measured IR laboratory spectra of two polycyclic aromatic nitrogen heterocycles (PANHs), quinoline ($C_9H_7N$) and phenanthridine ($C_{13}H_9N$), in solid argon and $H_2O$ at 15 K. These data are relevant to the search for aromatics in absorption along dense cloud lines of sight.

We find that some of the IR absorptions of quinoline have significantly different positions and intensities in $H_2O$ than in an argon matrix. In contrast, the IR spectrum of phenanthridine is, like normal PAHs, relatively insensitive to the presence of $H_2O$.

These divergent responses from quinoline and phenanthridine are not yet understood, so at present the only way to predict the IR absorptions of a PANH in interstellar dense clouds is to measure spectra of that molecule in solid $H_2O$. We are attempting to improve our understanding of the intermolecular interactions that govern the appearance of the IR spectra through theoretical modeling. It is to be hoped that this will free the community from the slow and onerous task of measuring the laboratory spectra of such molecules individually in $H_2O$.

REFERENCES

Allamandola, L. J., Hudgins, D. M., & Sandford, S. A. 1999, ApJ, 511, L115
Basile, B. P., Middleditch, B. S., & Oró, J. 1984, Organic Geochem., 5, 211
Bernstein, M. P., Sandford, S. A., & Allamandola, L. J. 2005, ApJ, in press
Bregman, J. D., Hayward, T. L., & Sloan, G. C. 2000, ApJ, 544, L75
Bregman, J. D., & Temi, P. 2001, ApJ, 554, 126
Brooke, T. Y., Sellgren, K., & Geballe, T. R. 1999, ApJ, 517, 883
Brooke, T. Y., Sellgren, K., & Smith, R. G. 1996, ApJ, 459, 209
Chiar, J. E., Tielens, A. G. G. M., Whittet, D. C. B., Schutte, W. A., Boogert, A. C. A., Lutz, D., van Dishoeck, E. F., & Bernstein, M. P. 2000, ApJ, 537, 749
Cox, P., & Kessler, M. F., eds. 1999, The Universe as Seen by ISO (ESA SP-427; Noordwijk: ESA)
Destexhe, A., Smets, J., Adamowicz, L., & Maes, G. 1994, J. Phys. Chem., 98, 1506
Garrison, A. A., Mamantov, G., & Wehry, E. L. 1982, Appl. Spectrosc., 36, 348
Hony, S., Van Kerckhoven, C., Peeters, E., Tielens, A. G. G. M., Hudgins, D. M., & Allamandola, L. J. 2001, A&A, 370, 1030
Hudgins, D. M., & Allamandola, L. J. 2004, in ASP Conf. Ser. 309, Astrophysics of Dust, ed. A. N. Witt, G. C. Clayton, & B. T. Draine (San Francisco: ASP), 665
Hudgins, D. M., Sandford, S. A., Allamandola, L. J., & Tielens, A. G. G. M. 1993, ApJS, 86, 713

Jenniskens, P., & Blake, D. F. 1994, Science, 265, 753
Jenniskens, P., Blake, D. F., Wilson, M. A., & Pohorille, A. 1995, ApJ, 455, 389
Kuan, Y.-J., Huang, H.-C., Charnley, S. B., Markwick, A., Botta, O., Ehrenfreund, P., Kisiel, Z., & Butner, H. M. 2003, in 25th IAU Meeting, Joint Discussion 14, Formation of Cometary Material (San Francisco: ASP), 44
Mattioda, A. L., Hudgins, D. M., Bauschlicher, C. W., Jr., Rosi, M., & Allamandola, L. J. 2003, J. Phys. Chem. A, 107, 1486
Peeters, E., Hony, S., Van Kerckhoven, C., Tielens, A. G. G. M., Allamandola, L. J., Hudgins, D. M., & Bauschlicher, C. W. 2002, A&A, 390, 1089
Peeters, Z., Botta, O., Charnley, S. B., Ruiterkamp, R., & Ehrenfreund, P. 2003, ApJ, 593, L129
Pizzarello, S. 2001, Lunar Planet. Sci. Conf., 32, 1886
Ricca, A., Bauschlicher, C W., & Bakes, E. L. O. 2001, Icarus, 154, 516
Sandford, S. A., Bernstein, M. P., & Allamandola, L. J. 2004, ApJ, 607, 346
Sellgren, K., Brooke, T. Y., Smith, R. G., & Geballe, T. R. 1995, ApJ, 449, L69
Sephton, M. A. 2002, Nat. Prod. Rep., 19, 292
Smith, R. G., Sellgren, K., & Tokunaga, A. T. 1989, ApJ, 344, 413
Snow, T. P., & Witt, A. N. 1995, Science, 270, 1455
Stoks, P. G., & Schwartz, A. W. 1982, Geochim. Cosmochim. Acta, 46, 309
Van Kerckhoven, C., et al. 2000, A&A, 357, 1013